Journal of Applied Fluid Mechanics, Vol. 12, No. 1, pp. 1-10, 2019.
Available online at www.jafmonline.net, ISSN 1735-3572, EISSN 1735-3645.
DOI: 10.29252/jafm.75.253.28744

Laminar Forced Convection and Entropy Generation of ZnO-Ethylene Glycol Nanofluid Flow through Square Microchannel with using Two-Phase Eulerian-Eulerian Model

C. Uysal[1†], K. Arslan[2] and H. Kurt[3]

[1] *Automotive Technologies Program, TOBB Vocational School of Technical Sciences, Karabuk University, Karabuk, 78050, Turkey*
[2] *Mechanical Engineering Department, Faculty of Engineering, Karabuk University, Karabuk, 78050, Turkey*
[3] *Mechanical Engineering Department, Faculty of Engineering and Architecture, Necmettin Erbakan University, Konya, 42140, Turkey*

†*Corresponding Author Email: cuneytuysal@karabuk.edu.tr*

(Received December 30, 2017; accepted July 28, 2018)

ABSTRACT

In this paper, convective heat transfer and entropy generation of ZnO-EG nanofluid flow through a square microchannel are numerically investigated. Flow is modelled by using Eulerian-Eulerian two phase flow model. Nanoparticle volume fraction of ZnO-EG nanofluid ranged between %1.0 and %4.0. As a result, it is found that the convective heat transfer coefficient of flow increased from 9718.15 W/m^{2}K to 23010.79 W/m^{2}K when 4.0% ZnO nanoparticle addition to pure EG at Re=100. Total entropy generation of ZnO-EG nanofluid decreases with increase in nanoparticle volume fraction of ZnO-EG nanofluid. It is also observed that the Bejan number decreases with increase in nanoparticle volume fraction of ZnO-EG nanofluid.

Keywords: Entropy generation; Ethylene glycol; Eulerian; Microchannel; Nanofluid; Two-phase.

NOMENCLATURE

A	area
A	coefficient defined in Eqs. 23
B	coefficient defined in Eqs. 22
Be	Bejan number
C_d	drag coefficient
C_P	specific heat
d_p	particle diameter
div	divergence
D_h	hydraulic diameter
f	darcy friction factor
F	force
$grad$	gradient
G	particle-particle interaction modulus
h	convective heat transfer coefficient
k	conductive heat transfer coefficient
L	length
$\dot{m}$	mass flow rate
Nu	Nusselt number
P	pressure
Pr	Prandtl number
q''	heat flux
Re	Reynolds number
$\dot{S}'_{gen}$	entropy generation rate per unit length
T	temperature
$\vec{V}$	velocity vector
β	friction factor
Γ	coefficient defined in Eqs. 21
μ	dynamic viscosity
ρ	density
ϕ	volumetric fraction
τ	shear stress
ω	coefficient defined in Eqs. 24

1. INTRODUCTION

Thermal management techniques provide better heating and cooling technology and high efficient thermal systems are very important for energy saving and efficiency. One of these techniques is the improving thermophysical properties of heat transfer fluids. The searches for this reason finally revealed "nanofluids". Nanofluid is a suspension obtained with dispersion of nano-sized metallic or non-metallic solid particles into conventional working liquids such as water, ethylene glycol or oil. The nanofluid term is firstly introduced by Choi in 1995.

In the last decade, many researches have numerically and experimentally investigated the convective heat transfer and fluid flow characteristics of nanofluids. In numerical analysis, the nanofluids flows are modeled as single-phase flow generally. This is because of that nanoparticles dispersed to base fluid has smaller diameter than 100 nm. However, some papers showed that the results obtained for nanofluid flows modeled using two-phase model are in better agreement with experimental data compared to that of single-phase model. Behzadmehr *et al.* (2007) modelled the turbulent convective heat transfer of Cu-water nanofluid flow through a circular tube using two-phase mixture model. They reported that two-phase mixture model is more precise than that of single-phase model. Kumar and Puranik (2017) also reported that Lagrangian-Eulerian two-phase modeling of turbulent forced convection of water based Al_2O_3, TiO_2 and Cu nanofluids gives more accurate results compared to that of single phase modeling for nanoparticle volume fractions smaller than 0.5%. For higher nanoparticle volume fractions, it is on the contrary. Moraveji and Ardehali (2013) compared the single-phase model with volume of fluid, mixture and Eulerian two-phase models for laminar forced convection of Al_2O_3-water nanofluid flow through minichannel heat sink. They reported that two-phase models are more precise by comparison with experimental reference data than single-phase data. Kalteh *et al.* (2011) numerically investigated laminar forced convection of Cu-water nanofluid flow through isothermally heated microchannel by using Eulerian-Eulerian two-phase modeling. It is found that relative velocity and temperature between phases is negligible. In addition, the obtained results for convective heat transfer enhancement with two-phase modeling are higher compared to that of single-phase and convective heat transfer enhancement increases with decrease in nanoparticle diameter. Mahdavi *et al.* (2015) separately applied the discrete phase model in the Lagrangian approach and mixture model in the Eulerian approach to water based Al_2O_3, SiO_2 and ZrO_2 nanofluid flows through vertical tube under laminar flow conditions. As a result, they recommended the discrete phase model due to its strength and simplicity. Moreover, the pressure loss results obtained for nanoparticle volume fractions less than 3% is more reliable in the discrete phase model. Siavashi and Jamali (2016) investigated the turbulent convective heat transfer and entropy generation of TiO2-water nanofluid flow through annuli for different radius ratios with same cross sectional area. The flow was modeled with mixture two-phase model. They expressed that radius ratio has an important effect on entropy generation rate and there is an optimal Reynolds number to minimize entropy generation rate.

Contrary to literature mentioned above, some studies reported that the results obtained for single-phase is more precise than that of two-phase or that single and two-phase models shows similar predictions. Moraveji and Esmaeili (2012) studied laminar forced convection heat transfer of Al_2O_3-water nanofluid through a circular tube under constant heat flux with using single and two-phase models. They reported that single and two-phase models give quite similar results. Akbari *et al.* (2012) compared six different combination of viscosity and thermal conductivity for single-phase modeling of turbulent forced convection of Al_2O_3-water nanofluid and then determined the most appropriate model with experimental results within them. Moreover, same problem is modeled as two-phase flow with volume of fluid, mixture and Eulerian models. It is reported that selected single-phase model is more appropriate compared to two-phase models for their study conditions. Behroyan *et al.* (2015) compared five different models, which are Newtonian and non-Newtonian single-phase models and mixture, Eulerian-Eulerian, Eulerian-Lagrangian models, for turbulent forced convection of Cu-water nanofluid flow. As a result, they recommended Newtonian single-phase and Eulerian-Lagrangian two-phase models due to their precise results.

Farzaneh *et al.* (2016) used constructal theory to investigate the using of microchannels with/without loops for cooling process of a square electronic component with internal heat generation. They aimed reducing the thermal resistance in their study. They reported that the maximum dimensionless temperature is reduced by 10% and 20%, while the maximum dimensionless pressure drop is decreased by 25% and 33% for one and two branch reverting microchannels, in comparison with the case without a branch. Ramiar *et al.* (2012) numerically solved conjugate heat transfer problem for a mixture flow of 60% ethylene glycol and 40% water in mass containing Al_2O_3 nanoparticles in two dimensional microchannel. They reported that using solid regions with higher thermal conductivities enhance heat transfer by increasing Nusselt number and amplify axial conduction effect. Farzaneh *et al.* (2017) studied the effect of reverting microchannels inside a heat sink having circular, square and triangular configurations for geometrical optimization. They founded that square geometry has the least thermal resistance.

In this study, laminar forced convection and entropy generation of ZnO-EG nanofluid flow having different nanoparticle volume fractions through a square microchannel are numerically investigated. The flow is modeled with Eulerian-Eulerian two-phase model. The results such as convective heat transfer coefficient, Nusselt number, pressure drop, Darcy friction factor and entropy generation for different nanoparticle volume fraction of ZnO-EG nanofluid are presented and compared.

2. MODEL CONFIGURATION

2.1 Geometrical Configuration

Convective heat transfer characteristics and entropy generation of ZnO-EG nanofluid through a square microchannel are numerically investigated. The flow is modeled as Eulerian-Eulerian two phase model. The hydraulic diameter of microchannel is assumed to be D_h= 150 μm. This means that dimension of each side of microchannel cross-section is 150 μm. The microchannel length is assumed to be 50 mm. The schematic diagram of microchannel investigated in this study is illustrated in Figure 1.

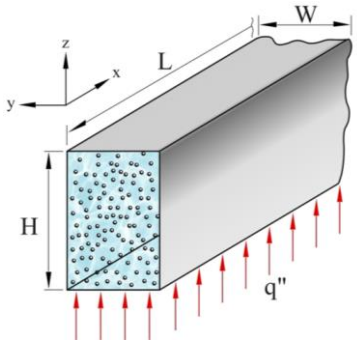

Fig. 1. Schematic diagram of microchannel considered in this study.

2.2 Governing Equations

There are three different Eulerian-Eulerian multiphase, which are the volume of fluid model, the mixture model and the Eulerian model. The volume of fluid model has not separate governing equations for solid and fluid phases. In addition, it is designed for two or more immiscible fluids. The mixture and the Eulerian models have different governing equations for solid and fluid phases. In this study, Eulerian model is selected for analyses due to that it allows considering granular temperature, solid-phase shear and bulk viscosities.

In Eulerian-Eulerian two-phase modeling; mass, momentum and energy equations are separately written for each phases, while the pressure is shared by all phases. The governing equations for particle and liquid phases can be written as follows (ANSYS Fluent, 2009):

$$\nabla(\rho_l\phi_l\vec{V}_l)=0 \tag{1}$$

$$\nabla(\rho_p\phi_p\vec{V}_p)=0 \tag{2}$$

$$\nabla(\rho_l\phi_l\vec{V}_l\vec{V}_l)=-\phi_l\nabla P + \nabla\left[\phi_l\mu_l\left(\nabla\vec{V}_l+\nabla\vec{V}_lT\right)\right]+F_d+F_{vm} \tag{3}$$

$$\nabla(\rho_p\phi_p\vec{V}_p\vec{V}_p)=-\phi_p\nabla P + \nabla\left[\phi_p\mu_p\left(\nabla\vec{V}_p+\nabla\vec{V}_pT\right)\right]-F_d+F_{vm}+F_{col} \tag{4}$$

$$\nabla(\rho_l\phi_lC_{p,l}T_l\vec{V}_l)=\nabla\left[\phi_lk_{eff,l}\nabla T_l\right]-h_v(T_l-T_p) \tag{5}$$

$$\nabla(\rho_p\phi_pC_{p,p}T_p\vec{V}_p)=\nabla\left[\phi_pk_{eff,p}\nabla T_p\right]+h_v(T_l-T_p) \tag{6}$$

where the subscripts l and p denote liquid and particle phases, respectively. In these equations, the following relation is valid.

$$\phi_l+\phi_p=1 \tag{7}$$

where ϕ is the volumetric fraction of liquid or particle phases. The momentum equations are including drag force (F_d), virtual mass force (F_{vm}) and collision force (F_{col}). The drag force between the phases is expressed as follows:

$$F_d=-\beta(\vec{V}_l-\vec{V}_p) \tag{8}$$

where β is friction coefficient. For two-phase flows with ϕ_l >0.8, β is calculated by following relation:

$$\beta=\frac{3}{4}C_d\frac{\phi_l(1-\phi_l)}{d_p}\rho_l\left|\vec{V}_l-\vec{V}_p\right|\phi_l^{-2.65} \tag{9}$$

where C_d is the drag coefficient and is expressed with following equation (Schiller and Naumann, 1935):

$$C_d=\begin{cases}\frac{24}{Re_p}\left(1+0.15\,Re_p^{\,0.687}\right) & Re_p<1000\\ 0.44 & Re_p\geq 1000\end{cases} \tag{10}$$

where Re_p is the particle Reynolds number and is calculated by using following equation:

$$Re_p=\frac{\phi_l\rho_l\left|\vec{V}_l-\vec{V}_p\right|d_p}{\mu_l} \tag{11}$$

where ρ and μ are density and dynamic viscosity, respectively. d_p is particle diameter. Virtual mass force is related with relative acceleration between two phases and is found by following equation:

$$F_{vm}=0.5\phi_p\rho_l\frac{D}{Dt}(\vec{V}_l-\vec{V}_p) \tag{12}$$

Collision force is related with particle-particle interaction and can be calculated with following relation:

$$F_{col}=G(\phi_l)\nabla\phi_l \tag{13}$$

where G is the particle-particle interaction modulus and is expressed with following relation:

$$G=1.0\,exp\left(-600\left[\phi_l-0.376\right]\right) \tag{14}$$

The h_v term expressed in Equation 6 and 7 is the volumetric interphase convective heat transfer coefficient and is expressed for mono-dispersed

spherical particles as follows (Kuipers *et al.*, 1992):

$$h_v = \frac{6(1-\phi_l)}{d_p} h_p \tag{15}$$

where h_p is the liquid-particle heat transfer coefficient and can be calculated with following relation (Ranz and Marshall, 1952):

$$Nu_p = \frac{h_p d_p}{k_l} = 2 + 1.1 Re_p^{0.6} Pr^{1/3} \tag{16}$$

where Pr is the Prandtl number of liquid phase. The k_{eff} expressed in Equations 5 and 6 denotes the effective thermal conductivity coefficient of liquid and particle phases and is written as follows, respectively (Kuipers *et al.*, 1992).

$$k_{eff,l} = \frac{k_{b,l}}{\phi_l} \tag{17}$$

$$k_{eff,p} = \frac{k_{b,p}}{\phi_p} \tag{18}$$

where,

$$k_{b,l} = \left(1 - \sqrt{(1-\phi_l)}\right) k_l \tag{19}$$

$$k_{b,p} = \sqrt{(1-\phi_l)}\left(\omega A + [1-\omega]\Gamma\right) k_l \tag{20}$$

The Γ coefficient is defined as follows:

$$\Gamma = \frac{2}{\left(1-\frac{B}{A}\right)} \left\{ \frac{B(A-1)}{A\left(1-\frac{B}{A}\right)^2} ln\left(\frac{A}{B}\right) - \frac{(B-1)}{\left(1-\frac{B}{A}\right)} - \frac{B+1}{2} \right\} \tag{21}$$

where A, B and ω coefficient can be expressed for spherical particles as follows:

$$B = 1.25 \left(\frac{[1-\phi_l]}{\phi_l} \right)^{10/9} \tag{22}$$

$$A = \frac{k_p}{k_l} \tag{23}$$

$$\omega = 7.26 \times 10^{-3} \tag{24}$$

2.3 Heat Transfer and Fluid Flow Relations

The Reynolds number is defined as follows:

$$Re = \frac{\rho_l u D_h}{\mu_l} \tag{25}$$

The local convective heat coefficient is expressed as follows:

$$h_x = \frac{q''}{(T_w - T_m)} \tag{26}$$

where T_w and T_m are wall and mean temperatures, respectively. The mean temperature for two-phase flows can be calculated by using following equation (Kalteh *et al.*, 2011):

$$T_m = \frac{\sum_{i=1}^{p} \left(\iint \rho_i u_i C_{p,i} T_i dA \right)}{\sum_{i=1}^{p} \left(\iint \rho_i u_i C_{p,i} dA \right)} \tag{27}$$

where the integration is realized on the cross-section of channel geometry. The local Nusselt number is defined as follows:

$$Nu_x = \frac{h_x D_h}{k_l} \tag{28}$$

The local Darcy friction factor can be written as follows:

$$f_x = \frac{8\tau_x}{\rho u^2} \tag{29}$$

where τ_x is shear stress of flow. The average values of convective heat transfer coefficient, Nusselt number and Darcy friction factor are calculated with following equations, respectively.

$$h = \frac{1}{A} \int_A h_x dA \tag{30}$$

$$Nu = \frac{1}{A} \int_A Nu_x dA \tag{31}$$

$$f = \frac{1}{A} \int_A f_x dA \tag{32}$$

For internal flow, the entropy generation per unit length can be written as follows (Bejan, 1982):

$$\dot{S}'_{gen,total} = \frac{q''^2 \pi D_h^2}{k T_b^2 Nu} + \frac{8\dot{m}^3 f}{\pi^2 \rho^2 T_b D_h^5} \tag{33}$$

In Eqs. 33, the first term on the right side expresses entropy generation per unit length due to heat transfer and the second term expresses entropy generation per unit length due to fluid friction.

The Bejan number is formulated as follows:

$$Be = \frac{\dot{S}'_{gen,heat\ transfer}}{\dot{S}'_{gen,heat\ transfer} + \dot{S}'_{gen,\ fluid\ friction}} \tag{34}$$

and it is defined as the ratio of entropy generation due to heat transfer to total entropy generation.

2.4 Boundary Conditions

A constant heat flux of 1000 W/m^2 is applied to bottom surface of microchannel. The inlet temperature and velocity distributions of both phases are assumed as uniform and both phases enter to channel same inlet temperature and velocity. The inlet temperature of both phases is assumed to be 300 K. The inlet velocities of both phases are calculated by specified Reynolds number (Re =10-100) with Equation 25. The diameter of ZnO nanoparticles is d_p =18 nm. In microchannel outlet, pressure outlet boundary condition is applied for both phases.

2.5 Numerical Procedure

The governing equations mentioned above for both

phases are discretized by using finite volume method in the view of boundary conditions. In the computational domain, a non-uniform grid is employed. In the region close to microchannel walls, finer grids are used. For the convective and diffusive terms the first order upwind method is used. For solving velocity-pressure coupling, the Phase Coupled SIMPLE (Semi Implicit Method for Pressure Linked Equations) method is used. The convergence criterion is selected to be 10^{-6} for this study.

2.6 Grid Independency Test and Code Validation

The grid independency test is performed to avoid the effect of grid number on the results obtained with numerical procedure. Six different grid numbers ranging from 40000 to 1400000 are used. Same grid numbers are used for each aspect ratio of rectangular microchannel. The selection of optimum grid numbers is realized by considering the change of results with grid numbers. The calculations are realized for the model having selected optimum grid number.

To validate the accuracy of the numerical model, the results obtained by numerical computation is compared with the numerical results for two-phase model presented by Moraveji and Ardehali (2013) and with experimental results presented by Ho and Chen (2013). The comparison of the results obtained by this study with the results presented in the literature is shown in Figure 2.

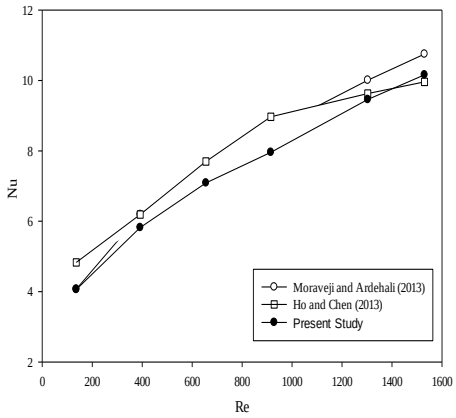

Fig. 2. Mesh accuracy test.

The results obtained by this study show good agreement with the results presented by Moraveji and Ardehali (2013) and Ho and Chen (2013). The average deviation between the results obtained by this study and Moraveji and Ardehali (2013) is 1.52%, while it is 7.55% for the results presented by Ho and Chen (2013).

3. Results And Discussion

The convective heat transfer characteristics and entropy generation of ZnO-EG nanofluid flow through a square microchannel are numerically investigated by using Eulerian-Eulerian two-phase model. The Reynolds number is in the range of 10 and 100. Constant heat flux of q'' = 1000 W/m^2 is applied to the bottom surface of the microchannels.

The velocity distributions of ZnO-EG nanofluid flow for different nanoparticle volume fractions in the outlet cross-section of square microchannel and lateral section of inlet region of square microchannel are shown in Figure 3 and 4, respectively.

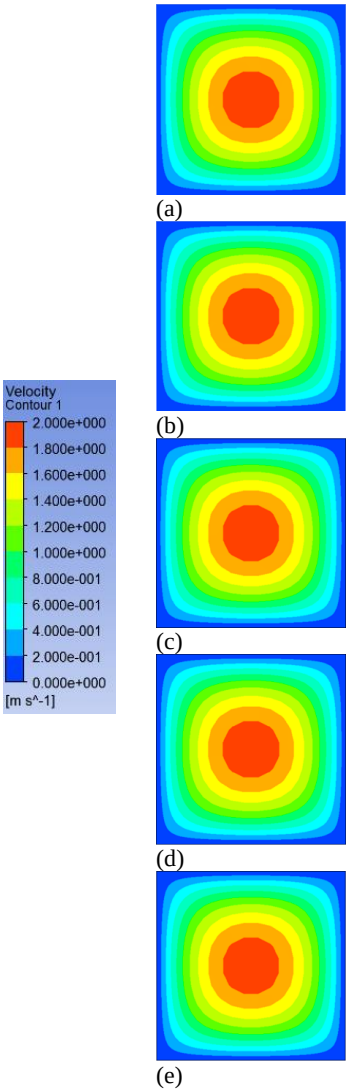

Fig. 3. Velocity distribution of outlet section of square microchannel for different nanoparticle volume fractions of ZnO-EG nanofluid (a) ϕ_p =0, (b) ϕ_p =1.0%, (c) ϕ_p =2.0%, (d) ϕ_p =3.0% and (e) ϕ_p =4.0%.

The temperature distributions of ZnO-EG nanofluid flow for different nanoparticle volume fractions in the outlet cross-section and outlet lateral section of square microchannel are shown in Figure 5 and 6, respectively.

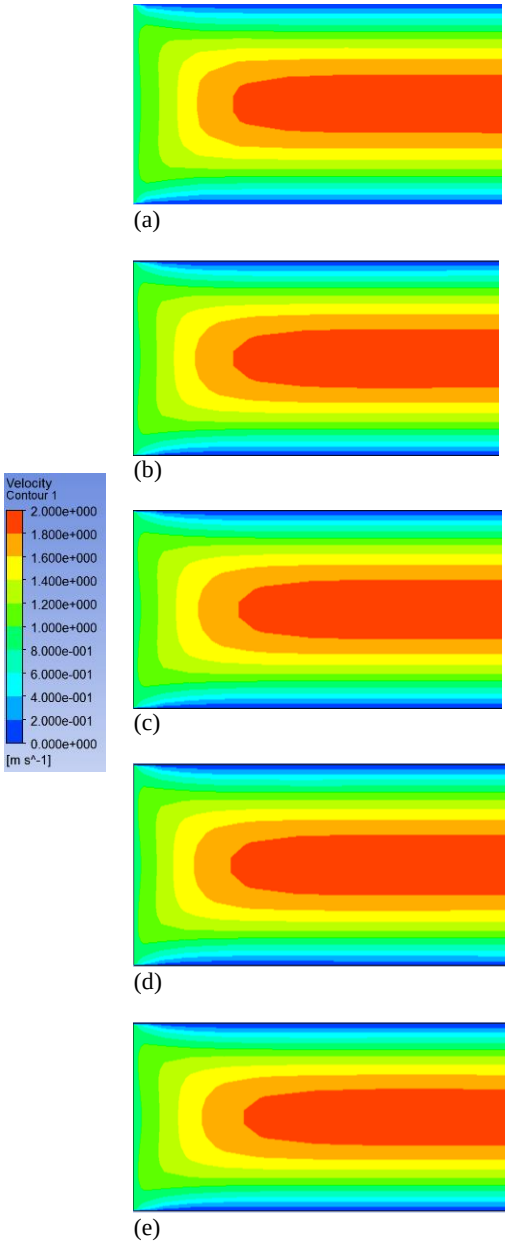

Fig. 4. Velocity distribution of lateral section of inlet region of square microchannel for different nanoparticle volume fractions of ZnO-EG nanofluid (a) ϕ_p =0, (b) ϕ_p =1.0%, (c) ϕ_p =2.0%, (d) ϕ_p =3.0% and (e) ϕ_p =4.0%.

As can be seen from Figure 5 and 6, wall temperature of ZnO-EG nanofluid decreases with increase in nanoparticle volume fraction of ZnO-EG nanofluid. Moreover, it can be observed that increase in nanoparticle volume fraction of ZnO-EG nanofluid causes to increase in bulk temperature of ZnO-EG nanofluid.

The variation of average convective heat transfer coefficient of ZnO-EG nanofluid flow with the Reynolds number is illustrated in Figure 7.

As can be seen from Figure 7, the convective heat transfer coefficient increases with increase in nanoparticle volume fraction of ZnO-EG nanofluid and in the Reynolds number. The maximum convective heat transfer coefficient for this study is obtained to be 23010.79 W/m^{2}K at Re = 100 for ZnO-EG nanofluid having nanoparticle volume fraction of 4.0%. Whereas, the convective heat transfer coefficient obtained for pure EG at Re = 100 is 9718.15 W/m^{2}K. The reason of increment in convective heat transfer coefficient with nanoparticle addition is due to that the difference between wall and bulk temperatures of nanofluid decreases with increase in nanoparticle addition.

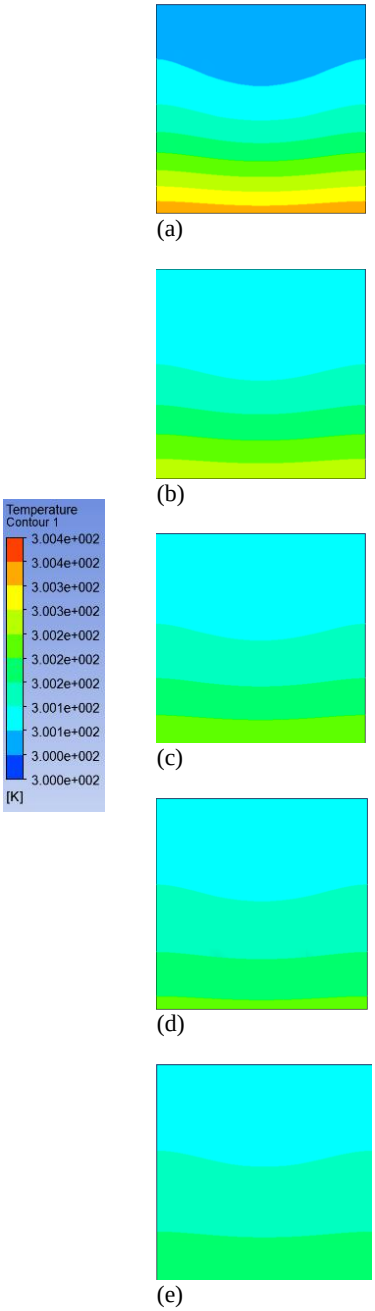

Fig. 5. Temperature distribution of outlet section of square microchannel for different nanoparticle volume fractions of ZnO-EG nanofluid (a) ϕ_p =0, (b) ϕ_p =1.0%, (c) ϕ_p =2.0%, (d) ϕ_p =3.0% and (e) ϕ_p =4.0%.

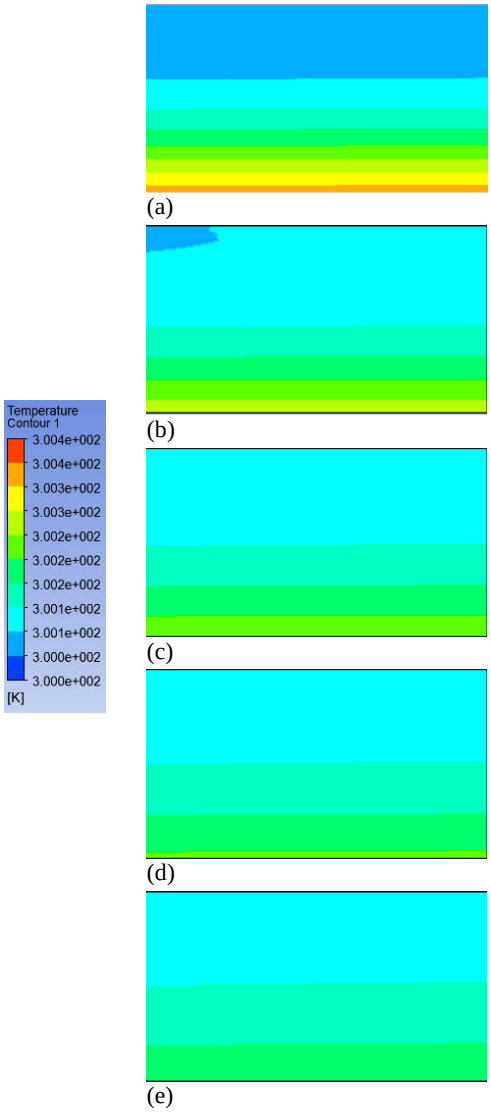

Fig. 6. Temperature distribution of lateral section of inlet region of square microchannel for different nanoparticle volume fractions of ZnO-EG nanofluid (a) ϕ_p =0, (b) ϕ_p =1.0%, (c) ϕ_p =2.0%, (d) ϕ_p =3.0% and (e) ϕ_p =4.0%.

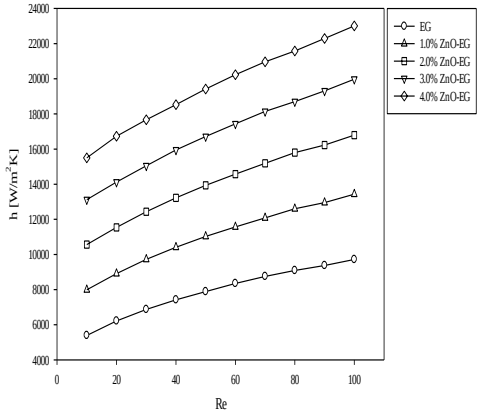

Fig. 7. Convective heat transfer coefficient.

The variation of the Nusselt number of ZnO-EG nanofluid flow with the Reynolds number is shown in Figure 8.

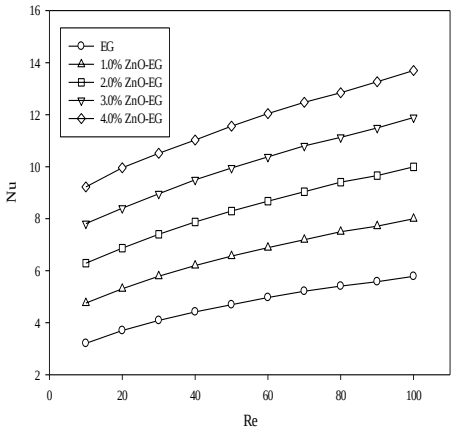

Fig. 8. Nusselt number.

The Nusselt number of ZnO-EG nanofluid flow increases with increasing nanoparticle volume fraction and the Reynolds number. The Nusselt number is already related with the convective heat transfer coefficient. Therefore, similar results are also obtained for the Nusselt number. At Re = 100, the Nusselt number obtained for ZnO-EG nanofluid having nanoparticle volume fraction of 4.0% is 13.7, while it is 5.78 for pure EG.

The variation of pressure drop of ZnO-EG nanofluid with the Reynolds number is illustrated in Figure 9.

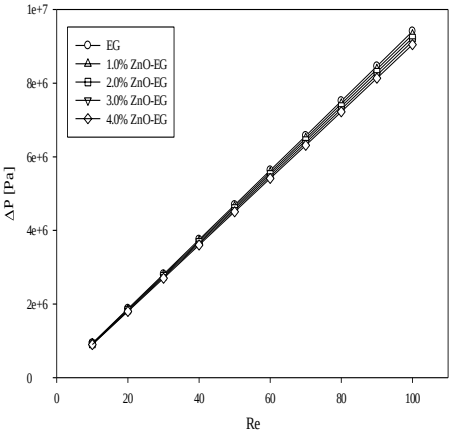

Fig. 9. Pressure drop.

It is clearly seen from Figure 9 that the pressure drop decreases with increase in nanoparticle volume fraction of ZnO-EG nanofluid. The pressure drop obtained for ZnO-EG nanofluid having nanoparticle volume fraction of 4.0% is 3.98% and 3.85 lower compared to that of pure EG at Re = 10 and Re = 100, respectively. However, for same microchannel geometry, Uysal *et al.* (2016) reported that ZnO nanoparticle addition of 4.0% to EG increases pressure drop 28.96% and 29.23% at Re=10 and Re=100, respectively, in single phase consideration. Suganthi *et al.* (2014) showed that ZnO nanoparticle addition to EG cause a reduction in viscosity due to that hydrogen bonding network of

ethylene glycol is reorganized with ZnO nanoparticle addition. It may be reason for decrease in pressure drop for two-phase approach.

The variation of Darcy friction factor of ZnO-EG nanofluid with the Reynolds number is illustrated in Figure 10.

The Darcy friction factor of ZnO-EG nanofluid decreases with increasing nanoparticle volume fraction of ZnO-EG nanofluid. This is due to that the pressure drop decreases with increase in nanoparticle volume fraction of ZnO-EG nanofluid and the Darcy friction factor is directly related with pressure drop.

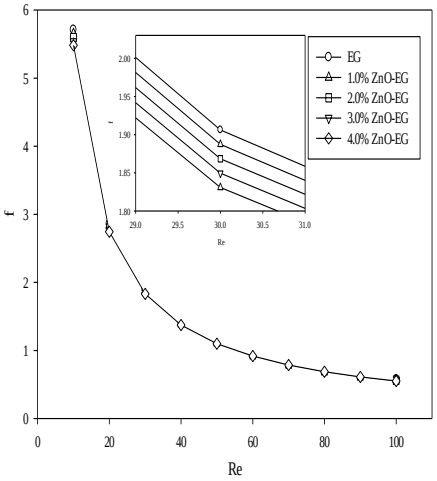

Fig. 10. Darcy friction factor.

The variation of entropy generation per unit length due to heat transfer with the Reynolds number is shown in Figure 11.

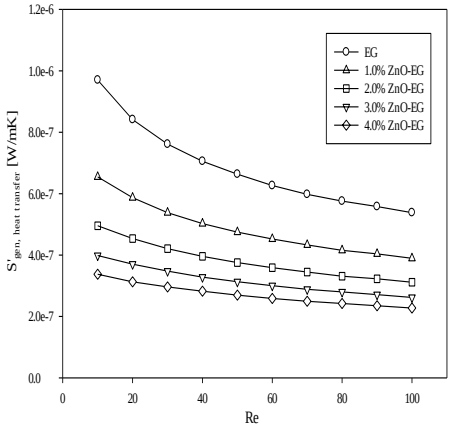

Fig. 11. Entropy generation due to heat transfer.

As can be seen from Figure 11, entropy generation due to heat transfer decreases with increase in the Reynolds number. This decrement tendency decreases with increase in nanoparticle volume fraction of ZnO-EG nanofluid. It is also found that entropy generation due to heat transfer decreases with increase in nanoparticle volume fraction of ZnO-EG nanofluid. At Re=10, entropy generation due to heat transfer values obtained for pure EG and ZnO-EG nanofluid having nanoparticle volume fraction of 4.0% are 9.7031×10^{-7} W/mK and 3.3748×10^{-7} W/mK, respectively. Whereas, entropy generation values due to heat transfer of 5.3848×10^{-7} W/mK and 2.2742×10^{-7} W/mK are obtained for pure EG and 4.0% ZnO-EG nanofluid, at Re=100, respectively.

The variation of entropy generation per unit length due to fluid friction with the Reynolds number is shown in Figure 12.

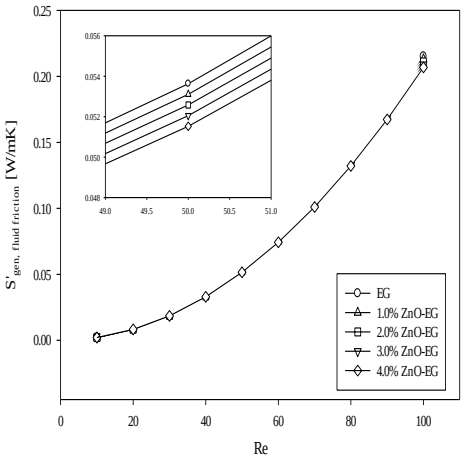

Fig. 12. Entropy generation due to fluid friction.

Entropy generation due to fluid friction increases with increase in the Reynolds number. In addition, it decreases with increase in nanoparticle volume fraction of ZnO-EG nanofluid; this decrement is not significant. ZnO nanoparticle of 4.0% addition to pure EG decreases the entropy generation due to fluid friction from 0.002139 W/mK to 0.002053 W/mK and from 0.2151 W/mK to 0.2068 W/mK at Re = 10 and Re =100, respectively.

The variation of total entropy generation per unit length with the Reynolds number is illustrated in Figure 13.

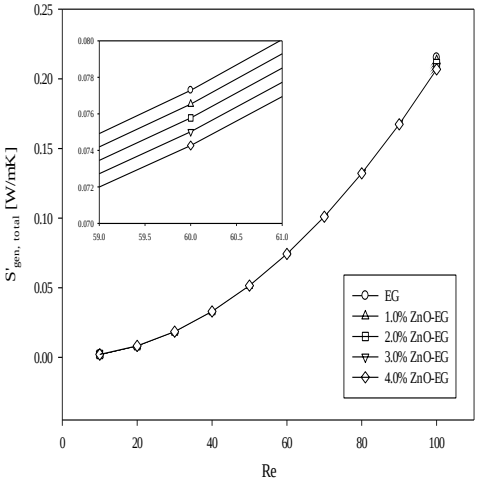

Fig. 13. Total entropy generation.

Same results with entropy generation due to fluid friction are obtained for total entropy generation. This is due to that the obtained values for entropy generation due to heat transfer are negligible compared to that of entropy generation due to fluid friction. The microchannel considered in this study has a micro-sized hydraulic diameter. This case causes to that entropy generation due to fluid friction is dominant.

The variation of the Bejan number with the Reynolds number is shown in Figure 14.

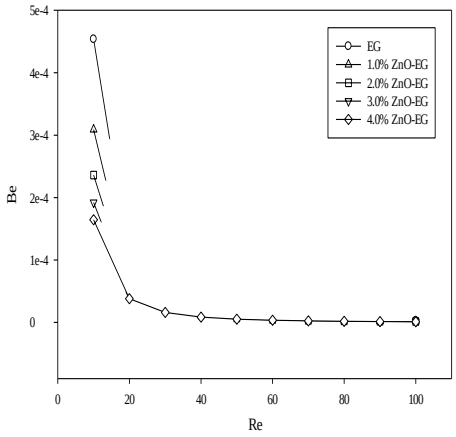

Fig. 14. Bejan number.

As can be seen from Figure 14, Bejan number decreases with increase in Reynolds number and nanoparticle volume fraction of ZnO-EG nanofluid. ZnO nanoparticle addition to pure EG decreases the contribution of entropy generation due to heat transfer in the total entropy generation.

4. CONCLUSION

In this study, laminar forced convection and entropy generation of ZnO-EG nanofluid flow through square microchannel are numerically investigated. The flow is modelled by using Eulerian-Eulerian two-phase model. Results showed that 4.0% ZnO nanoparticle addition to pure EG causes to high increment of 187.36% at Re=10 and of 136.78% at Re=100 in convective heat transfer coefficient. Similar high increments in convective heat transfer coefficient and in Nusselt number are reported by Moraveji and Ardehali (2013) for Al_2O_3/water nanofluid flow. ZnO nanoparticle addition to pure EG causes to decrease in wall temperature. This leads to increment in convective heat transfer coefficient and in Nusselt number. This may be due to that nanoparticles inside flow destroyed the boundary layer.

Entropy generation due to heat transfer decreases with increase in nanoparticle volume fraction of ZnO-EG nanofluid, while entropy generation due to fluid friction increases. For this study, entropy generation due to heat transfer can be neglect when it is compared with entropy generation due to fluid friction. This is due to that microchannel considered in this study has small hydraulic diameter. Researchers and/or engineers should focus on fluid friction to decrease entropy generation for thermal management of microchannel applications.

REFERENCES

Akbari, M., N. Galanis and A. Behzadmehr (2012). Comparative assessment of single and two-phase models for numerical studies of nanofluid turbulent forced convection. *International Journal of Heat and Fluid Flow.* 37, 136-146.

ANSYS Fluent (2009). ANSYS Fluent 12.0 Theory Guide, ANSYS Inc.

Behroyan, I., P. Ganesan, S. He and S. Sivasankaran (2015). Turbulent forced convection of Cu-water nanofluid: CFD model comparison. *International Communications in Heat and Mass Transfer.* 67, 163-172.

Behzadmehr, A., M. Saffar-Avval and N. Galanis (2007). Prediction of turbulent forced convection of a nanofluid in a tube with uniform heat flux using a two phase approach. *International Journal of Heat and Fluid Flow.* 28, 211-219.

Bejan, A. (1982). Entropy Generation through Heat and Fluid Flow. John Wiley and Sons: New York.

Choi, S. U. S. (1995). Enhancing thermal conductivity of fluids with nanoparticles. *ASME FED.* 231, 99-103.

Farzaneh, M., M. R. Salimpour and M. R. Tavakoli (2016). Design of bifurcating microchannels with/without loops for cooling of square-shaped electronic components. *Applied Thermal Engineering.* 108, 581-595.

Farzaneh, M., M. R. Tavakoli and M. R. Salimpour (2017). Effect of reverting channels on heat transfer performance of microchannels with different geometries. *Journal of Applied Fluid Mechanics* 10, 41-53.

Ho, C. J. and W. C. Chen (2013). An experimental study on thermal performance of Al_2O_3/water nanofluid in a minichannel heat sink. *Applied Thermal Engineering.* 50, 516-522.

Kalteh, M., A. Abbassi, M. Saffar-Avval and J. Harting (2011). Eulerian-Eulerian two-phase numerical simulation of nanofluid laminar forced convection in a microchannel. *International Journal of Heat and Fluid Flow.* 32, 107-116.

Kuipers, J., W. Prins and W. Van Swaaij (1992). Numerical calculation of wall-to-bed heat-transfer coefficients in gas-fluidized beds. *AICHE J.* 38, 1079-1091.

Kumar, N. and B. P. Puranik (2017). Numerical study of convective heat transfer with nanofluids in turbulent flow using a

Lagrangian-Eulerian approach. *Applied Thermal Engineering.* 111, 1674-1681.

Mahdavi, M., M. Sharifpur and J.P. Meyer (2015). CFD modelling of heat transfer and pressure drops for nanofluids through vertical tubes in laminar flow by Lagrangian and Eulerian approaches. *International Journal of Heat and Mass Transfer.* 88, 803-813.

Moraveji, M. K. and E. Esmaeli (2012). Comparison between single-phase and two-phases CFD modeling of laminar forced convection flow of nanofluids in a circular tube under constant heat flux. *International Communications in Heat and Mass Transfer.* 39, 1297-1302.

Moraveji, M. K. and R. M. Ardehali (2013). CFD modeling (comparing single and two-phase approaches) on thermal performance Al_2O_3/water nanofluid in mini-channel heat sink. *International Communications in Heat and Mass Transfer.* 44, 157-164.

Ramiar, A., A. A. Ranjbar and S. F. Hosseinizadeh (2012). Effect of axial conduction and variable properties on two-dimensional conjugate heat transfer of Al_2O_3-EG/water mixture nanofluid in microchannel. *Journal of Applied Fluid Mechanics.* 5, 79-87.

Ranz, W. and W. Marshall (1952). Evaporation from drops. *Chem. Eng. Prog*. 48, 141-146.

Schiller, L. and A. Naumann (1935). A drag coefficient correlation. *Vdi Zeitung.* 77, 318-320.

Siavashi, M. and M. Jamali (2016). Heat transfer and entropy generation analysis of turbulent flow of TiO_2-water nanofluid inside annuli with different radius ratios using two-phase mixture model. *Applied Thermal Engineering.* 100, 1149-1160.

Suganthi, K. S., V. L. Vinodhan and K. S. Rajan (2014). Heat transfer performance and transport properties of ZnO-ethylene glycol and ZnO-ethylene glycol-water nanofluid coolants. *Applied Energy.* 135, 548-559.

Uysal, C., K. Arslan and H. Kurt (2016). A numerical analysis of fluid flow and heat transfer characteristics of ZnO-Ethylene glycol nanofluid in rectangular microchannels. *Strojniski Vestnik-Journal of Mechanical Engineering.* 62, 603-613.